Delay-throughput curves for timer-based OBS burstifiers with light load

M. Izal, J. Aracil, D. Morató and E. Magaña
Departamento de Automática y Computación
Universidad Pública de Navarra, Pamplona, SPAIN
mikel.izal@unavarra.es

Abstract—**The OBS burstifier delay-throughput curves are analyzed in this paper. The burstifier incorporates a timer-based scheme with minimum burst size, i. e., bursts are subject to padding in light-load scenarios. Precisely, due to this padding effect, the burstifier normalized throughput may not be equal to unity. Conversely, in a high-load scenario, padding will seldom occur. For the interesting light-load scenario, the throughput-delay curves are derived and the obtained results are assessed against those obtained by trace-driven simulation. The influence of long-range dependence and instantaneous variability is analyzed to conclude that there is a threshold timeout value that makes the throughput curves flatten out to unity. This result motivates the introduction of adaptive burstification algorithms, that provide a timeout value that minimizes delay, yet keeping the throughput very close to unity. The dependence of such optimum timeout value with traffic long-range dependence and instantaneous burstiness is discussed. Finally, three different adaptive timeout algorithms are proposed, that tradeoff complexity versus accuracy.**

Keywords: **Burstification algorithms, performance evaluation of OBS networks**

I. Introduction and problem statement

Optical Burst Switching is a transfer mode that is halfway between circuit switching and packet switching, thus providing intermediate switching granularity. It is based on unconfirmed resource reservation for the optical burst, which is composed by several IP packets. Due to the fact that an optical burst is significantly larger than a single packet the technological requirements at the optical switches are less stringent. For example, receiver synchronization is easier to achieve for a burst (milliseconds transmission time) than for a packet (nanoseconds transmission time). The same applies to switching time requirements.

The functional unit in charge of producing optical bursts out of packets is denoted *burstifier.* Precisely, a number of burstification algorithms have been proposed and analyzed [1], [2], [3], [4], [5], [6]. In [5], three categories are identified: i) time-based algorithms, ii) burst-length-based algorithms and mixed time/burst-length algorithms. Time-based algorithms take a fixed assembly time as a primary criterion to create a burst, whereas burst-length based algorithms take the burst length instead. The third category corresponds to hybrid schemes that consider both time and burst length, whichever is fulfilled first. In a light load scenario, a burst-length-based algorithm results in a high packetization delay, due to the time it takes to collect a sufficient number of packets to create a burst [5]. For such scenario, time-based schemes are significantly more efficient, since the packetization delay is given by the assembly time. In this paper, we will focus on light-load scenarios and time-based schemes. The case with no padding has been considered elsewhere [7]. On the other hand, in [8] the latency and mean burst size are derived for an OBS network *with acknowledgments*. In those references padding is not considered and the packet arrival process is assumed to be Poisson, not long-range dependent.

The burstification algorithm under consideration is as follows: the incoming packet stream is demultiplexed per destination in separate queues. A timer is started with the first packet arrival in a queue. Then, upon timer expiration, the optical burst is formed and relayed to the optical core. On the other hand, it should be noted that bursts cannot be arbitrarily small, due to the optical switches technological constraints (for example minimum switching time). Thus, there is a lower bound to the optical burst size b_{min} and padding will be required for some of the bursts.

In this paper, we study the impact of burst padding on the optical network throughput. We choose the *delay-throughput* curve as the performance metric. As the timeout value increases more packets are allowed to be transported onto the same optical burst and padding will be less frequent. However, as the timeout value increases so does the burstification delay. The findings of this paper allow to select a burstifier operating point that minimizes burstification delay, yet keeping throughput at a reasonable value. On the other hand, the impact of long-range dependence and instantaneous variability on the throughput-delay curve will be analyzed. Finally, we propose an adaptive timeout algorithm that minimizes delay while keeping throughput beyond a given threshold.

A. Assumptions

In a medium to heavily loaded OBS network, padding will not be likely to occur and the impact on throughput will be negligible in practice. However, a light load scenario will potentially produce many bursts with a number of packets below the minimum burst size and padding will be necessary. Even in highly loaded networks load fluctuations do happen, for instance during weekends, and light-load epochs will be observed[1]. For our analysis, the light-load assumption will imply that the lightpath bandwidth is very large in comparison to the incoming traffic average. When the timer expires, all packets awaiting transmission in the burst assembly queue are transmitted.

Secondly, the incoming traffic model (bytes per interval) will be modeled by a Fractional Gaussian Noise (FGN), which has been shown to model accurately traffic from a LAN [9]. While recent studies show that *highly multiplexed core traffic* may be modeled as a non-homogeneous Poisson process [10] note that

This work was funded by Spanish Ministry of Education and Science (projects CAPITAL TEC2004-05622-C04-04 and PINTA TEC2004-06437-C05-03)

[1] See for instance http://loadrunner.uits.iu.edu/weathermaps/abilene/ for daily variation of traffic in an Internet backbone

the burstifier *demultiplexes* traffic on a per-destination basis. On the other hand, burstifiers will be placed at the edges of the optical network and not at the core. As a result, the expected multiplex level is not as large. Furthermore, note that in order to calculate the throughput only the number of information bytes per burst matters and not the packet arrival dynamics, which may have multifractal behavior for low multiplex levels [11]. Precisely, the FGN is a fluid-flow model that provides the number of bytes per time interval only. While the small timescale traffic fluctuations are not captured by the model, the long-range dependence from interval to interval is indeed accurately portrayed. In this paper, we wish to analyze the impact of such dependence in the OBS throughput. Finally, our analytical results will be compared to trace-driven simulations, and the traffic model assumptions will be verified using a real-world scenario.

II. Analysis

According to our previous results in [12], for a timer-based burstifier, it turns out that the traffic arriving per time interval T_0 is a Gaussian random variable with mean $\mu = \mu' T_0$ and standard deviation $\sigma = \sigma' T_0^H$. Let us denote such random variable by X, with T_0 being the timeout value, H being the Hurst parameter, μ' and σ' being the mean and standard deviation of the marginal distribution of the traffic arriving in a given time unit (in this paper it will represent bytes arriving in a $1ms$ interval).

A. Delay-throughput curve

Let us assume that the minimum burst size is b_{min}. The throughput will be defined as the ratio between the information bits and the total bits transmitted. Thus, the throughput will equal unity whenever $X > b_{min}$ and $E[X]/b_{min}$ if $X < b_{min}$, where $E[X]$ denotes the expected value of random variable X. For convenience, let us define the random variable Y as the following function of X,

$$Y = \begin{cases} X & : \quad X \le b_{min} \\ b_{min} & : \quad X > b_{min} \end{cases} \tag{1}$$

then, the throughput is equal to

$$\rho = \frac{E[Y]}{b_{min}} \tag{2}$$

Note that the definition of Y implies that the throughput is equal to one if padding is not necessary ($Y = b_{min}$). As a result, Y is a truncated Gaussian random variable in the range $[0, b_{min}]$. Let $\phi(x) = \frac{1}{\sqrt{2\pi}} e^{-\frac{1}{2}x^2}$ and $\Phi(x) = \int_{-\infty}^{x} \phi(t)dt$. Then,

$$P(Y \le y) = \begin{cases} \Phi\left(\frac{y-\mu}{\sigma}\right) & : \quad y < b_{min} \\ 1 & : \quad y \ge b_{min} \end{cases} \tag{3}$$

and

$$\begin{aligned} E[Y] &= E\left[Y|Y < b_{min}\right] P(Y < b_{min}) + \\ &+ E\left[Y|Y = b_{min}\right] P(Y = b_{min}). \end{aligned} \tag{4}$$

In order to derive the conditional expectation $E\left[Y|Y < b_{min}\right]$ we use the Moment Generating Function (MGF)

$$M_Y(t) = E\left[e^{tY}|Y < b_{min}\right] = e^{\mu t + \frac{\sigma^2 t^2}{2}} \frac{\phi\left(\frac{b_{min}-\mu}{\sigma} - \sigma t\right)}{\phi\left(\frac{b_{min}-\mu}{\sigma}\right)} \tag{5}$$

yielding

$$E\left[Y|Y < b_{min}\right] = M_Y'(0) = \mu - \sigma \frac{\phi(\alpha)}{\Phi(\alpha)} \tag{6}$$

with $\alpha = \frac{b_{min}-\mu}{\sigma}$. Let us define the *hazard* function [2] as $\lambda(\alpha) = \frac{\phi(\alpha)}{1-\Phi(\alpha)}$. Then

$$E\left[Y|Y < b_{min}\right] = M_Y'(0) = \mu - \sigma\lambda(-\alpha) \tag{7}$$

and, using (4),

$$E[Y] = (\mu - \sigma\lambda(-\alpha))\,\Phi(\alpha) + b_{min}\left(1 - \Phi(\alpha)\right). \tag{8}$$

Now, use (2) to obtain the throughput expression. Figure 1 shows an example of throughput curve.

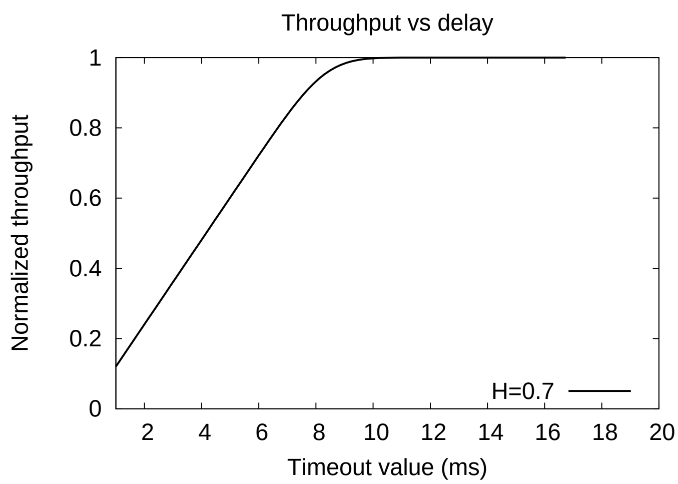

Fig. 1. Delay-throughput curve (parameters $b_{min} = 500$ Kbytes, $T_0 = 1 \ldots 20$, byte arrivals per ms with $\mu' = 60162.88$ bytes, $\sigma' = 15038.2$ bytes, $H = 0.73$,)

As expected, an increase in the timeout value results in a better throughput since more packets can be accommodated per burst. One may argue that the average delay a packet will experience is not the timeout value but actually half a timeout value. However, and without loss of generality, we will consider the maximum delay. Thus, the delay in the x-axis will be equal to the timeout value.

B. Generated load

In this section we derive an expression for the generated traffic to the OBS network. Due to padding, the burstifier traffic is larger than or equal to the input IP traffic. Let Z be the random variable that denotes the bits per second generated by the burstifier. Then,

[2] Or *inverse Mills ratio*

$$Z = \begin{cases} b_{min} & : \quad X \leq b_{min} \\ X & : \quad X > b_{min} \end{cases} \tag{9}$$

and,

$$P(Z \leq z) = \begin{cases} 0 & : \quad z < b_{min} \\ \Phi\left(\frac{z-\mu}{\sigma}\right) & : \quad z \geq b_{min} \end{cases} \tag{10}$$

i.e., Z is a truncated Gaussian variable from below. Now, we use the following MGF,

$$M_Z(t) = E\left[e^{tZ}|Z > b_{min}\right] = e^{\mu t + \frac{\sigma^2 t^2}{2}} \frac{1 - \phi\left(\frac{b_{min}-\mu}{\sigma} - \sigma t\right)}{1 - \phi\left(\frac{b_{min}-\mu}{\sigma}\right)} \tag{11}$$

and, thus,

$$E\left[Z|Z > b_{min}\right] = M'_Z(0) = \mu + \sigma\lambda(\alpha). \tag{12}$$

Finally,

$$\begin{aligned} E[Z] &= E\left[Z|Z = b_{min}\right] P(Z = b_{min}) + \\ &+ E\left[Z|Z > b_{min}\right] P(Z > b_{min}) = \\ &= b_{min}\phi(\alpha) + (\mu + \sigma\lambda(\alpha))(1 - \phi(\alpha)). \end{aligned} \tag{13}$$

and $E[Z]/T_0$ represents the rate in bps.

C. Validation

In this section we perform a trace driven simulation to validate the analytical results. We used the Abilene-I data set provided by NLANR [3]. The Abilene-I data set traces contain traffic from two OC-48 links, that was collected at the Indianapolis router node. Traces are 2 hours long, each of them comprises 12 files (10 minutes each) that contain the pair *(arrival time, packet size)* for every packet in the link. We use 10 minutes worth of traffic from a 2.5Gbps link as a real-world traffic source for the burstifier. The Abilene-I trace selected shows an average traffic rate around 480Mbps which, assuming a 10Gbps wavelength in the OBS port, makes the utilization factor be approximately equal to 0.05. Figure 2 shows one of the Abilene traces (10 minutes). The trace characteristics are summarized in table I [4].

μ' (bytes in $1ms$)	σ' (bytes in $1ms$)	H
60162.8786	15038.2	0.73

TABLE I
TRACE CHARACTERISTICS

From the packet arrival process, the burst arrival process is generated through simulation of a timer-based burstifier. Simulation is performed with a set of timeouts varying from 1 to 20 ms and several values of $b_{min} = \{100, 500, 900\}$ KBytes. The obtained throughput $\frac{E[Y]}{b_{min}}$ is plotted in figure 3, along with the theoretical results from (8).

[3] http://pma.nlanr.net/Traces/long/ipls1.html

[4] Packets were taken from the Illinois to Cleveland link (IPLS-CLEV-20020814-102000-1), on August 14th, 2002, from 10:20 to 10:30 AM

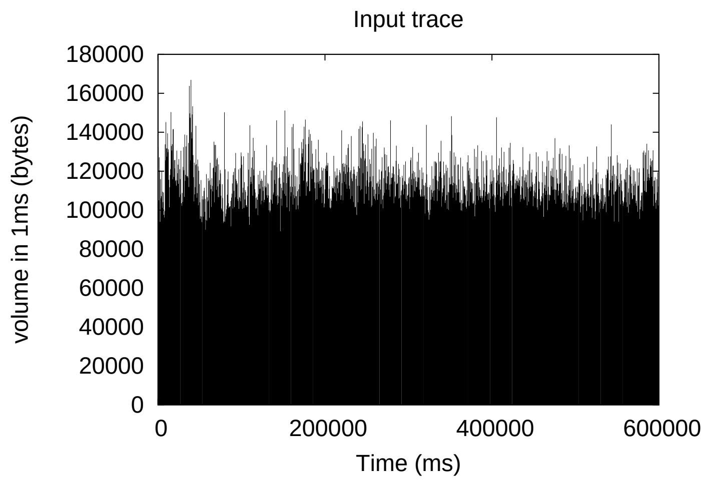

Fig. 2. Abilene-I trace

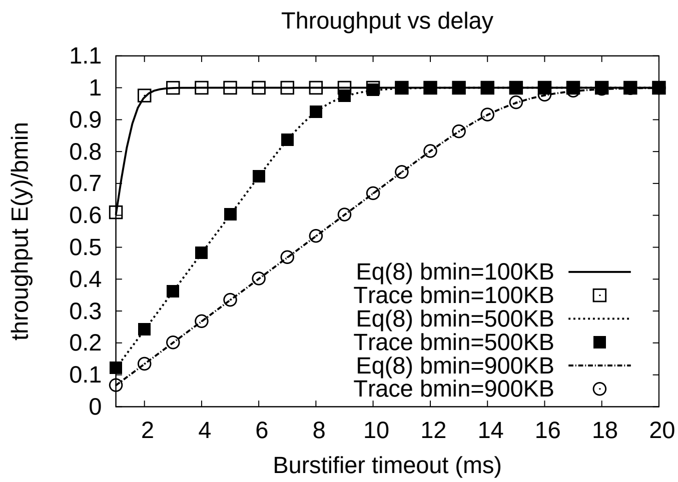

Fig. 3. Throughput-delay curve for the Abilene-I trace

Note that the theoretical curve matches very well the simulation values, thus validating the model and suggesting that Abilene-I traces are very well modeled by a FGN process, at least in the milliseconds scale. This is a timescale that is relevant for a burstifier with timeout values of milliseconds. Smaller timescales do not really matter, since the aggregation performed at the burstifier is not affected by the packet arrival dynamics below the timeout value timescale.

As the minimum burst size (b_{min}) increases the throughput decreases. For each value of b_{min} a cutoff timeout value exists that makes the throughput curves flatten out to unity.

On the other hand, figure 4 shows the generated load to the OBS network, showing that the analytical expressions match closely the trace-driven simulation results. The y-axis shows the traffic generated by the burstifier and the x-axis the timeout value, for different minimum burst sizes. Interestingly, note that the joint effect of low burstifier timeout and large minimum burst size can amplify the input traffic to 6 Gbps, more than 10 times the average input traffic (480 Mbps). As a result, it turns that b_{min} and T_{out} should be carefully selected. The throughput-delay expressions provided in the previous section serve to select a burstifier operating point that actually minimizes the padding effect (i.e. throughput values close to 1). Such operating point also guarantees that the burstifier offered rate to the OBS network is close to the input traffic rate.

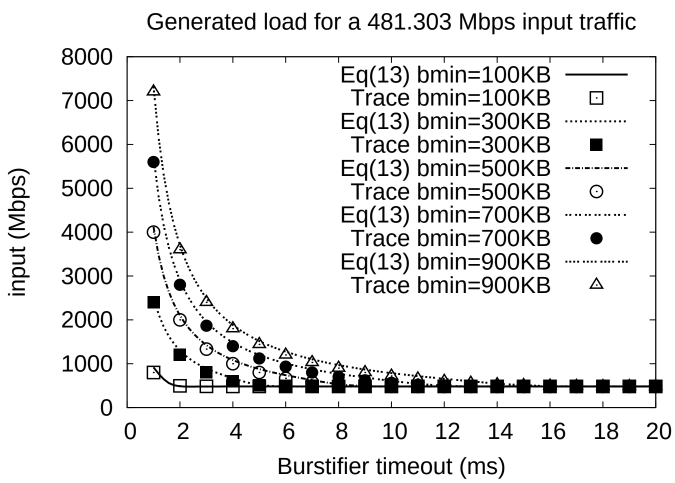

Fig. 4. Input traffic to the OBS network

III. Results and discussion

In this section we evaluate the impact of the incoming traffic parameters on the OBS throughput. First, the influence of long-range dependence on the throughput-delay features of the OBS burstifier will be analyzed. Then, the influence of the incoming traffic coefficient of variation will be studied. Finally, we will discuss whether dynamic burstification algorithms may serve to adaptively tune the burstifier timeout value in order to sustain throughput above a certain threshold.

A. Influence of long-range dependence on delay-throughput curves

The *Hurst parameter* H provides a measure of the traffic correlation structure. A value of $H = 0.5$ indicates no correlation (independent increments). As H increases, the traffic correlation also increases. Long-range dependence occurs whenever $1/2 < H < 1$. Figure 5 shows the delay-throughput curves derived in the previous section for different values of H and two extreme cases of minimum burst size, i.e. b_{min}=100 KBytes and b_{min}=900 KBytes.

As long-range dependence increases, the throughput decreases for a given delay value. On the other hand, the impact of long-range dependence on throughput is larger as the minimum burst size b_{min} increases. If the minimum burst size is large, padding will be performed more frequently. Overall, if the timeout value is larger than a certain threshold the effect of long-range dependence is negligible. This threshold is approximately equal to 20 ms in the worst-case of b_{min}=900 Kbytes. Below this timeout value the dependence on the value of H is

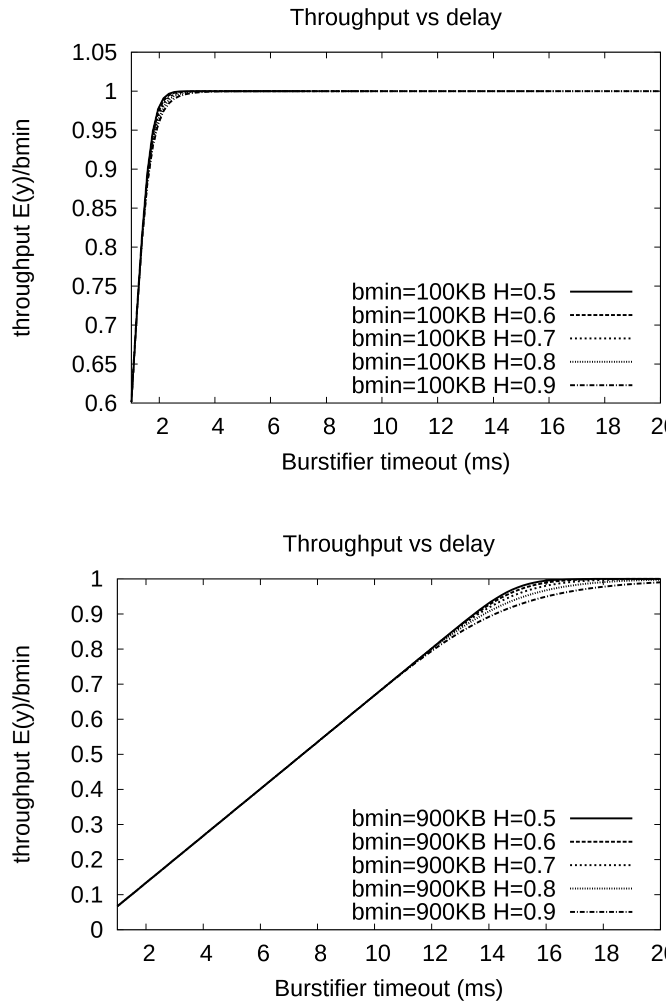

Fig. 5. Delay-throughput curves for different values of H (b_{min}=100 -top- and b_{min}=900 -bottom-)

higher but it is marginal compared with the dependence on the timeout value.

B. Influence of coefficient of variation on delay-throughput curves

The coefficient of variation ($c_v = \sigma/\mu$) provides a measure of the instantaneous variability of traffic. Note that this is "orthogonal" to the correlation. While long-range dependence serves to characterize the traffic behavior with time, the coefficient of variation is an instantaneous measure. Note also that the coefficient of variation depends on the scale of aggregation of the traffic process.

A sensitivity analysis of the throughput-delay curves versus the coefficient of variation is presented in this section. Figure 6 shows the delay-throughput curves for different values of c_v and two extreme cases of minimum burst size, i.e. b_{min}=100 KBytes and b_{min}=900 KBytes.

It turns out that larger values of c_v have negative influence on the throughput. The influence is worse the larger the minimum burst size value. As with long-range dependence, the impact

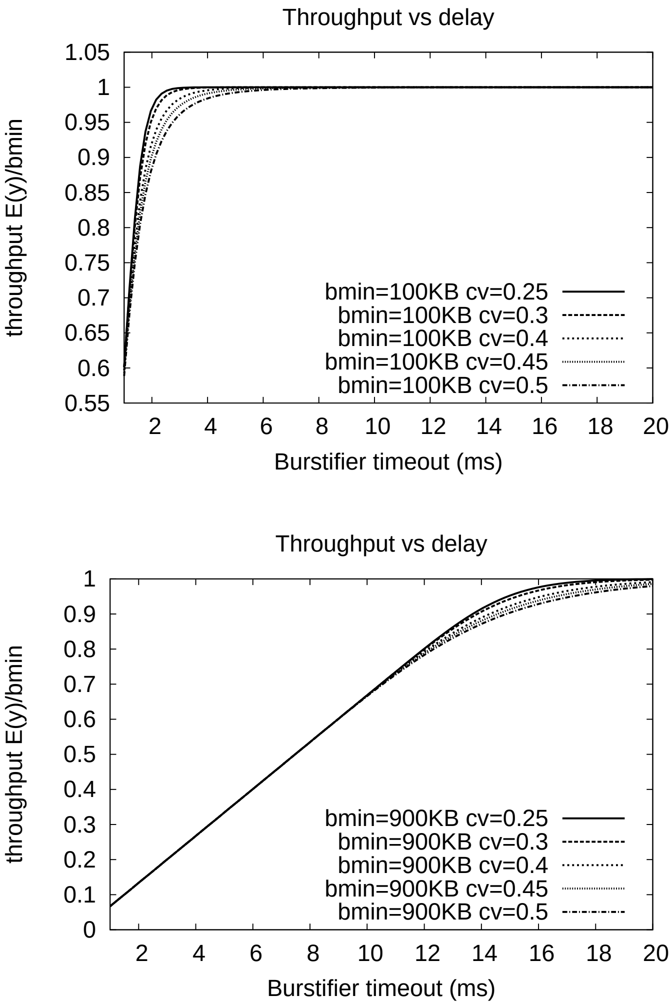

Fig. 6. Delay-throughput curves for different values of C_v (b_{min}=100 -top- and b_{min}=900 -bottom-)

of instantaneous variability on throughput is negligible beyond a certain timeout value. For a worst-case of b_{min}=900 Kbytes this threshold is also approximately equal to 20 ms.

C. *Dynamic adaptation of the timeout value*

The results of the previous section show a negative gradient of the throughput with both the coefficient of variation (instantaneous variability) and Hurst parameter (long-range dependence). However, there is a timeout value that makes such gradient be equal to zero. Such timeout value depends on the minimum burst size, the traffic load and, to a lesser extent, it also depends on the long-range dependence parameter H and the coefficient of variation c_v.

The above observation leads us to seek for an expression that provides the timeout value for which the delay throughout curves flatten out to unity. Not only this is beneficial to maximize the throughput at the minimum delay cost but also to decrease the network load. For the Abilene-I trace considered in section II-C, recall that the increased traffic load due to padding is shown in figure 4. The effect of choosing a wrong timeout value is very significant not only for the throughput, but also for the generated load to the OBS network.

Table II shows the threshold timeout value that provides a throughput equal to 95%. Our backbone traffic trace has a coefficient of variation equal to 0.25 for an aggregation interval of $1ms$. The same trace gives a $c_v = 0.054$ using intervals of $1s$ due to the decay of the variance with aggregation. In [9] the variance coefficient is equal to 0.34 (aggregation 1s) for a LAN traffic trace (trace *pOCT.TL*), showing higher variability in comparison with our trace. Actually, as the input traffic multiplex level increases, the coefficient of variation decreases. Note that OBS networks are expected to carry traffic from a large number of hosts.

The figures in table II show that for small values of the coefficient of variation, H has only a slight incremental influence on the timeout value, whereas for large values of the coefficient of variation the influence is much stronger. Thus, if input traffic has a small coefficient of variation then only estimation of the first and second moment is necessary. As the coefficient of variation increases one needs to take into account the influence of long-range dependence.

The fact that the delay-throughput curves are sensitive to both instantaneous burstiness and long-range dependence *only with large coefficient of variation* is very significant and useful for practical engineering purposes. Our findings show that if c_v is low only the traffic first and second moment need to be estimated in order to derive an optimal timeout value.

Concerning the change rate of the traffic moments, other proposals based on link state estimation assume that the network load remains stable in timescales of minutes [13]. If that is the case, one could devise an adaptive burstifier that would offer minimum delay and maximum throughput for any given input traffic stream. The timeout value rate of change would be in the scale of minutes, which seems reasonable from a practical implementation standpoint.

IV. ADAPTIVE TIMEOUT ALGORITHM FOR LONG-RANGE DEPENDENT TRAFFIC

In this section we propose three different adaptive timeout algorithms and compare them for different values of the Hurst parameter H and coefficient of variation c_v. The proposed algorithms tradeoff complexity versus accuracy.

A. *Load estimate (L-estimate)*

The load-based estimate T_0^L is based on the traffic first moment only, i. e.

$$T_0^L = \frac{b_{min}}{\hat{\mu}'} \tag{14}$$

being $\hat{\mu}'$ the input traffic rate estimate in bps. The basic assumptions is that the influence of the second moment and H parameter is negligible.

B. *Load-Variance estimate (LV-estimate)*

The load-variance estimate T_0^{LV} is based on the first and second moment. It is obtained as the solution of the following nonlinear program

TABLE II
BURSTIFIER TIMEOUT (MS) FOR 95% THROUGHPUT

bmin=100KB					
	cv=0.25	cv=0.32	cv=0.39	cv=0.45	cv=0.50
H=0.5	1.8	1.9	2.1	2.2	2.4
H=0.6	1.8	2.0	2.1	2.3	2.5
H=0.7	1.9	2.0	2.2	2.5	2.7
H=0.8	1.9	2.1	2.4	2.7	3.0
H=0.9	1.9	2.2	2.5	3.0	3.7
bmin=500KB					
	cv=0.25	cv=0.32	cv=0.39	cv=0.45	cv=0.50
H=0.5	8.1	8.3	8.4	8.6	8.7
H=0.6	8.2	8.4	8.7	8.9	9.2
H=0.7	8.4	8.7	9.1	9.5	9.8
H=0.8	8.7	9.1	9.7	10.4	11.1
H=0.9	9.1	9.8	10.9	12.2	13.8
bmin=900KB					
	cv=0.25	cv=0.32	cv=0.39	cv=0.45	cv=0.50
H=0.5	14.4	14.5	14.7	14.9	15.1
H=0.6	14.6	14.8	15.1	15.4	15.7
H=0.7	14.8	15.2	15.7	16.2	16.7
H=0.8	15.3	15.9	16.8	17.7	18.6
H=0.9	16.1	17.3	19.0	20.9	23.2

$$\begin{array}{ll} \text{Minimize} & T_0 \\ \text{subject to} & \rho(\hat{\mu}, \hat{\sigma}_{0.5}, \hat{\alpha}_{0.5}) \quad > 0.95 \end{array} \quad (15)$$

where $\hat{\mu} = \hat{\mu}' T_0$, $\hat{\sigma}_{0.5} = \hat{\sigma}' T_0^{0.5}$ and $\hat{\alpha}_{0.5} = \frac{b_{min} - \hat{\mu}}{\hat{\sigma}_{0.5}}$. The throughput $\rho(\hat{\mu}, \hat{\sigma}_{0.5}, \hat{\alpha}_{0.5}) = E[Y]/b_{min}$ can be obtained using (8). The LV-estimate neglects the influence of self-similarity (i.e. $H = 0.5$). Details for solving this problem and for parameter estimation with long-range dependence are given in the appendix.

C. *Load-Variance-H estimate (LVH-estimate)*

The load-variance-H estimate T_0^{LV} is based on the first, second moment and H parameter. It is obtained as the solution of the following nonlinear program

$$\begin{array}{ll} \text{Minimize} & T_0 \\ \text{subject to} & \rho(\hat{\mu}, \hat{\sigma}_{\hat{H}}, \hat{\alpha}_{\hat{H}}) \quad > 0.95 \end{array} \quad (16)$$

where $\hat{\mu} = \hat{\mu}' T_0$, $\hat{\sigma}_{\hat{H}} = \hat{\sigma}' T_0^{\hat{H}}$ and $\hat{\alpha}_{\hat{H}} = \frac{b_{min} - \hat{\mu}}{\hat{\sigma}_{\hat{H}}}$. Details for solving this problem are given in the appendix. This algorithm provides the best timeout value in comparison to the L-estimate and LV-estimate algorithms. However, this is at a cost of higher complexity in parameter estimation.

D. *Evaluation*

The proposed algorithms will be evaluated for input traffic with different dependence (H parameter) and instantaneous burstiness (coefficient of variation). The evaluation is performed under ideal conditions, i. e. it will be assumed that there is no estimation error in computing the parameters $\hat{\mu}', \hat{\sigma}'$. In what follows, we will focus on obtaining the minimum T_0 value that yields a throughput greater than 95%.

Note that table II already shows the T_0 values corresponding to algorithm LVH-estimate, with no estimation error. We take that table as a reference and calculate the following performance figures. First, the relative deviation from the optimum value of the L-estimate and LV-estimate is evaluated. Such relative deviation is defined as follows

$$\nu^x = \frac{|T_0^x - T_0^{LVH}|}{T_0^{LVH}} \quad (17)$$

where $x \in \{L, LV\}$ for the L-estimate and LV-estimate respectively. Secondly, the actual throughput that is obtained with both the L-estimate and the LV-estimate is calculated. Even though the target throughput is 95%, note that this will only be attained with the LVH estimate. Tables III and IV show the relative deviation ν^x for the L-estimate and LV-estimate.

Tables V and VI show the throughput obtained by a burstifier using either L-estimate or LV-estimate. With LV-estimate, the throughput does not fall below 85% even if the coefficient of variation is doubled from that of the original traffic. This holds true for the whole range of variation of H. On the other hand, the lowest attained throughput with a simpler L-estimate is 80%. This suggests that a simple estimate can drive a variable timeout burstifier to adapt the timeout so as to maintain a reasonably high throughput.

The tables show that for small coefficient of variation the L-estimate and LV-estimate produce timeout values that are very close to the theoretical optimal value. Since OBS networks are expected to multiplex traffic from a large number of sources this is actually the case. In order to verify this conclusion, we extensively analyze the Abilene-I data set. Table VII shows the H and c_v values (on the ms scale) for every trace in the Abilene-I data set. Note that all of them have a small coefficient of variation (c_v), which is usually below 0.3. On the other hand, the Hurst parameter (H) takes on values in the vicinity of 0.7. For $c_v = 0.25$ and $H = 0.7$, the timeout value that achieves a 95% throughput with minimum burst size $b_{min} = 500$ KB is equal to 8.4 ms. To derive such value one needs to solve the LVH-estimate program (16), that requires knowledge of first and second moments and Hurst parameter. The L-estimate provides a timeout equal to 8.5 ms and 94.7% throughput whereas for the LV-estimate the timeout is equal to 9 ms and the throughput is 93.5%. Even though the burstification delay is slightly increased and the throughput is a little less than 95%, note that only first moment estimation is needed for the L-estimate and first and second moment estimates are needed for the LV-estimate. Furthermore, the timeout value is straightforward to calculate with the L-estimate algorithm (equation 14).

V. CONCLUSIONS

In this paper we have derived the throughput-delay curve for a timer-based burstifier with minimum burst size. A threshold timeout value exists that makes the normalized throughput value

TABLE III

Relative deviation (percentage) of the L-estimate timeout ν^{L} (ms) with respect to the optimum value (LVH-estimate for) 95% throughput

bmin=100KB	cv=0.25	cv=0.32	cv=0.39	cv=0.45	cv=0.50
H=0.5	7.7%	12.5%	20.8%	24.4%	30.7%
H=0.6	7.7%	16.9%	20.8%	27.7%	33.5%
H=0.7	12.5%	16.9%	24.4%	33.5%	38.4%
H=0.8	12.5%	20.8%	30.7%	38.4%	44.6%
H=0.9	12.5%	24.4%	33.5%	44.6%	55.1%

bmin=500KB	cv=0.25	cv=0.32	cv=0.39	cv=0.45	cv=0.50
H=0.5	2.6%	0.1%	1.1%	3.4%	4.5%
H=0.6	1.4%	1.1%	4.5%	6.6%	9.7%
H=0.7	1.1%	4.5%	8.7%	12.5%	15.2%
H=0.8	4.5%	8.7%	14.3%	20.1%	25.1%
H=0.9	8.7%	15.2%	23.8%	31.9%	39.8%

bmin=900KB	cv=0.25	cv=0.32	cv=0.39	cv=0.45	cv=0.50
H=0.5	3.9%	3.2%	1.8%	0.4%	0.9%
H=0.6	2.5%	1.1%	0.9%	2.9%	4.7%
H=0.7	1.1%	1.6%	4.7%	7.7%	10.4%
H=0.8	2.2%	5.9%	11.0%	15.5%	19.6%
H=0.9	7.1%	13.5%	21.3%	28.4%	35.5%

TABLE IV

Relative deviation (percentage) of the LV-estimate timeout ν^{LV} (ms) with respect to the optimum value (LVH-estimate for) 95% throughput

bmin=100KB	cv=0.25	cv=0.32	cv=0.39	cv=0.45	cv=0.50
H=0.5	0.0%	0.0%	0.0%	0.0%	0.0%
H=0.6	0.0%	5.0%	0.0%	4.3%	4.0%
H=0.7	5.3%	5.0%	4.5%	12.0%	11.1%
H=0.8	5.3%	9.5%	12.5%	18.5%	20.0%
H=0.9	5.3%	13.6%	16.0%	26.7%	35.1%

bmin=500KB	cv=0.25	cv=0.32	cv=0.39	cv=0.45	cv=0.50
H=0.5	0.0%	0.0%	0.0%	0.0%	0.0%
H=0.6	1.2%	1.2%	3.4%	3.4%	5.4%
H=0.7	3.6%	4.6%	7.7%	9.5%	11.2%
H=0.8	6.9%	8.8%	13.4%	17.3%	21.6%
H=0.9	11.0%	15.3%	22.9%	29.5%	37.0%

bmin=900KB	cv=0.25	cv=0.32	cv=0.39	cv=0.45	cv=0.50
H=0.5	0.0%	0.0%	0.0%	0.0%	0.0%
H=0.6	1.4%	2.0%	2.6%	3.2%	3.8%
H=0.7	2.7%	4.6%	6.4%	8.0%	9.6%
H=0.8	5.9%	8.8%	12.5%	15.8%	18.8%
H=0.9	10.6%	16.2%	22.6%	28.7%	34.9%

TABLE V

Thoughput obtained using the L-estimate algorithm for a 95% target throughput

bmin=100KB	cv=0.25	cv=0.32	cv=0.39	cv=0.45	cv=0.50
H=0.5	92.3%	90.2%	88.0%	86.2%	84.5%
H=0.6	91.9%	89.7%	87.4%	85.4%	83.7%
H=0.7	91.5%	89.2%	86.7%	84.7%	82.9%
H=0.8	91.0%	88.6%	86.0%	83.9%	82.0%
H=0.9	90.6%	88.0%	85.3%	83.0%	81.0%

bmin=500KB	cv=0.25	cv=0.32	cv=0.39	cv=0.45	cv=0.50
H=0.5	96.6%	95.6%	94.6%	93.8%	93.1%
H=0.6	95.7%	94.6%	93.4%	92.4%	91.4%
H=0.7	94.7%	93.3%	91.8%	90.5%	89.4%
H=0.8	93.5%	91.7%	89.9%	88.3%	86.9%
H=0.9	92.0%	89.8%	87.5%	85.6%	83.9%

bmin=900KB	cv=0.25	cv=0.32	cv=0.39	cv=0.45	cv=0.50
H=0.5	97.4%	96.7%	96.0%	95.4%	94.8%
H=0.6	96.6%	95.7%	94.8%	94.0%	93.2%
H=0.7	95.6%	94.4%	93.1%	92.1%	91.1%
H=0.8	94.2%	92.7%	91.0%	89.6%	88.4%
H=0.9	92.4%	90.4%	88.2%	86.4%	84.8%

TABLE VI

Throughput obtained using the L-estimate algorithm for a 95% target throughput

bmin=100KB	cv=0.25	cv=0.32	cv=0.39	cv=0.45	cv=0.50
H=0.5	95.5%	95.2%	95.8%	95.3%	95.8%
H=0.6	95.0%	94.6%	95.0%	94.3%	94.6%
H=0.7	94.5%	93.9%	94.1%	93.2%	93.3%
H=0.8	94.0%	93.2%	93.2%	92.0%	91.8%
H=0.9	93.5%	92.4%	92.1%	90.6%	90.1%

bmin=500KB	cv=0.25	cv=0.32	cv=0.39	cv=0.45	cv=0.50
H=0.5	95.2%	95.6%	95.1%	95.3%	95.0%
H=0.6	94.4%	94.5%	93.9%	93.8%	93.4%
H=0.7	93.5%	93.3%	92.3%	92.0%	91.3%
H=0.8	92.3%	91.7%	90.3%	89.7%	88.7%
H=0.9	90.8%	89.7%	87.9%	86.8%	85.4%

bmin=900KB	cv=0.25	cv=0.32	cv=0.39	cv=0.45	cv=0.50
H=0.5	95.2%	95.0%	95.1%	95.2%	95.3%
H=0.6	94.5%	94.1%	93.9%	93.8%	93.7%
H=0.7	93.6%	92.8%	92.3%	91.9%	91.5%
H=0.8	92.3%	91.2%	90.2%	89.4%	88.8%
H=0.9	90.7%	89.0%	87.5%	86.2%	85.1%

TABLE VII

H AND c_v (MILLISECONDS TIMESCALE) FOR ABILENE-I TRACES (EACH FILE COMPRISES 10 MINUTES WORTH OF TRAFFIC)

Abilene trace file name	H	c_v
IPLS-CLEV-20020814-090000-0.gz	0.68	0.28
IPLS-CLEV-20020814-091000-0.gz	0.74	0.32
IPLS-CLEV-20020814-092000-0.gz	0.76	0.32
IPLS-CLEV-20020814-093000-0.gz	0.75	0.31
IPLS-CLEV-20020814-094000-0.gz	0.75	0.29
IPLS-CLEV-20020814-095000-0.gz	0.72	0.29
IPLS-CLEV-20020814-100000-0.gz	0.74	0.29
IPLS-CLEV-20020814-101000-0.gz	0.75	0.28
IPLS-CLEV-20020814-102000-0.gz	0.71	0.27
IPLS-CLEV-20020814-103000-0.gz	0.73	0.29
IPLS-CLEV-20020814-104000-0.gz	0.73	0.31
IPLS-CLEV-20020814-105000-0.gz	0.68	0.29
IPLS-CLEV-20020814-090000-1.gz	0.78	0.28
IPLS-CLEV-20020814-091000-1.gz	0.75	0.26
IPLS-CLEV-20020814-092000-1.gz	0.73	0.25
IPLS-CLEV-20020814-093000-1.gz	0.80	0.26
IPLS-CLEV-20020814-094000-1.gz	0.73	0.25
IPLS-CLEV-20020814-095000-1.gz	0.73	0.25
IPLS-CLEV-20020814-100000-1.gz	0.72	0.25
IPLS-CLEV-20020814-101000-1.gz	0.76	0.27
IPLS-CLEV-20020814-102000-1.gz	0.74	0.25
IPLS-CLEV-20020814-103000-1.gz	0.73	0.25
IPLS-CLEV-20020814-104000-1.gz	0.75	0.26
IPLS-CLEV-20020814-105000-1.gz	0.71	0.25

equal to unity. Such threshold value depends on the instantaneous traffic burstiness and long-range dependence to a much lesser extent than on the traffic load and minimum burst size. On the other hand, a bad choice of timeout value results in a severe increase of network load (see figure 4)

Three adaptive timeout algorithms have been proposed that tradeoff accuracy versus complexity. Our trace-driven analysis of the Abilene backbone shows that for most cases of real Internet traffic a first moment estimation is enough to provide a timeout value very close to the optimum. Thus, an adaptive timeout algorithm can be easily incorporated to timer-based burstifiers, with a significant benefit in burstification delay and throughput.

APPENDIX

A. *Solving the nonlinear programs (15) and (16)*

It can be easily shown that the constraint function in both programs (15) and (16) is increasing and concave. Let us denote the constraint function by f. The value of T_0 can be approximatted by the single zero of the function $f - 0.95$. Such zero can be found using a search method (for instance, Fibonacci search).

B. *Moment and Hurst parameter estimation with long-range dependent traffic*

Note that programs (15) and (16) require estimation of the input traffic mean, variance and Hurst parameter (only for program (16)). Let $(X_1, \ldots, X_n)$ be n traffic samples. Since traffic shows long-range dependence the correlation function can be approximatted by $\rho(k) \sim k^{2H-2}$. The well known variance estimator $s^2 = \frac{1}{n-1}\sum_{i=1}^{n}(X_i - \overline{X})^2$, where $\overline{X} = \frac{1}{n}\sum_{i=1}^{n} X_i$ is biased due to the covariance terms involved in the calculation.

A variance estimate has been proposed by the authors in [14], that provides a confidence interval on the variance estimate. Such estimator is defined as follows

$$s'^2 = \frac{1}{n/r - 1}\sum_{i=1}^{n/r}(X_{ri} - \overline{X'(n,r)})^2 \tag{18}$$

being r a parameter and being $\overline{X'(n,r)}$ the r-decimated mean $\overline{X'(n,r)} = 1/(n/r)\sum_{i=1}^{n/r} X_{ri}$. This estimator allows confidence intervals on the sample variance, for small values of r ($r > 4$).

For on-line estimation of the traffic average, in presence of long-range dependence, see [15]. Percival shows that if one is interested in estimating the mean in a given time frame this can be achieved by decimation at a moderate decrease in efficiency. Finally, a wavelets-based on-line Hurst parameter estimation, has been proposed in [16].

REFERENCES

[1] A. Ge, F. Callegati, and L. S. Tamil. On optical burst switching and self-similar traffic. *IEEE Communications Letters*, 4(3):98–100, March 2000.

[2] X. Yu, Y. Chen, and C. Qiao. Study of traffic statistics of assembled burst traffic in optical burst switched networks. In *Proceedings of Opticomm 2002*, pages 149–159, 2002.

[3] K. Laevens. Traffic characteristics inside optical burst switched networks. In *Proceedings of Opticomm 2002*, pages 137–148, 2002.

[4] S. Oh and M. Kang. A burst assembly algorithm in optical burst switching networks. In *Proceedings of OFC*, pages 771–773, 2002.

[5] Yu X, J.Li, X. cao, Y. Chen, and C. Qiao. Traffic statistics and performance evaluation in optical burst switched networks. *IEEE/OSA Journal of Lightwave Technology*, 22(11):2722– 2738, December 2004.

[6] M. de Vega Rodrigo and J. Gotz. An analytical study of optical burst switching aggregation strategies. In *Proceedings of Broadnets 2004, workshop on OBS*, San Jose, California, 2004.

[7] R. Rajaduray, S. Ovadia, and D. Blumenthal. Analysis of an edge router for span-constrained optical burst switched (obs) networks. *IEEE Journal of Lightwave Technology*, 11(22):2693–2705, November 2004.

[8] A. Zalesky, E. W. M. Wong, M. Zukerman, H. Le Vu, and R. S. Tucker. Performance analysis of an obs edge router. *IEEE Photonics Technology Letters*, 16(2):695–697, February 2004.

[9] I. Norros. On the use of Fractional Brownian Motion in the theory of connectionless networks. *IEEE Journal on Selected Areas in Communications*, 13(6):953–962, August 1995.

[10] T. Karagiannis, M. Molle, M. Faloutsos, and A. Broido. A nonstationary poisson view of internet traffic. In *Proceedings of IEEE INFOCOM 2004*, 2004.

[11] V. Ribeiro R. Riedi and R. Baraniuk. A multifractal wavelet model with application to network traffic. *IEEE Transactions on Information Theory*, 45:992–1018, April 1999.

[12] M. Izal and J. Aracil. On the influence of self similarity on optical burst switching traffic. In *Proceedings of GLOBECOM 2002*, 2002.

[13] S. K. Tan, G. Mohan, and K. C. Chua. Link scheduling state information based offset management for fairness improvement in wdm optical burst switching networks. *Computer Networks*, 45(6):819–834, August 2004.

[14] J. Aracil. A sampling technique for variance estimation of long-range dependent traffic. *IEEE Communication Letters*, 8(9):591–593, September 2004.

[15] D. B. Percival. On the sample mean and variance of a long-memory process. Technical Report 69, Department of Statistics, University of Washington, Seattle, 1985.

[16] A. Veitch M. Roughan and P. abry. Real-time estimation of the parameters of long-range dependence (extended version). *IEEE/ACM Transactions on Networking*, 8(4):467–478, August 2000.